NON-RESONANT MICROWAVE DISCHARGE START-UP IN HELIOTRON J

Yu.V. Kovtun[1], K. Nagasaki[2], S. Kobayashi[2], T. Minami[2], S. Kado[2], S. Ohshima[2], Y. Nakamura[3], A. Ishizawa[3], S. Konoshima[2], T. Mizuuchi[2], H. Okada[2], H. Laqua[4], T. Stange[4]

[1]*Institute of Plasma Physics, National Science Center*
"Kharkov Institute of Physics and Technology", Kharkiv, Ukraine;
[2]*Institute of Advanced Energy, Kyoto Univ., Uji, Kyoto 611-0011, Japan;*
[3]*Graduate School of Energy Science, Kyoto Univ. Uji, Kyoto 611-0011, Japan;*
[4]*Max-Planck Institute for Plasma Physics, 17491 Greifswald, Germany*

E-mail: Ykovtun@kipt.kharkov.ua

The non-resonant microwave discharge in strong magnetic fields was investigated in Heliotron J under the condition, $\omega_{ce}/\omega_{MW}>1$ (ω_{ce} and ω_{MW} are the angular electron cyclotron frequency and the angular microwave frequency, respectively). Following the production of a non-resonant microwave discharge plasma, it undergoes several phases in sequence: breakdown and formation of pre-ionized plasma, increase in linear and nonlinear phases of plasma density, and quasi-stationary stage. Several modes of non-resonant microwave discharge were investigated. In the power-scanning mode in non-resonant microwave discharge, a higher plasma density than that in the constant-power mode is achieved. The maximum average density achieved in the experiments is substantially greater than the critical density for O-wave (ordinary waves) $7.45 \cdot 10^{16}$ m^{-3} and can reach the value of $2.5 \cdot 10^{18}$ m^{-3}.
PACS: 52.50.Sw; 52.55.Hc

INTRODUCTION

Microwave discharges (MD) are widely used in physics research and applied plasma technologies [1-3]. They can be realized both in a magnetic field and without a magnetic field. Microwave discharges in a magnetic field at frequencies ω_{MW} multiple of the electron cyclotron frequency ω_{ce} ($\omega_{MW} = n\omega_{ce}$, n number harmonic) – electron cyclotron resonance (ECR) discharges – are common in controlled thermonuclear fusion research [4, 5]. In this research, ECR discharges are used to form and heat the high-temperature plasma. MD can also be used to form a plasma in strong magnetic fields under the condition, $\omega_{ce}/\omega_{MW} > 1$ [6, 7]. In this case, the achieved plasma density is higher than the critical density, N_c. Such non-resonant MD has been used to form a pre-ionized plasma for subsequent neutral beam injection (NBI) on Heliotron J [8-11]. In these experiments, a microwave generator was used at a frequency of 2.45 GHz and the ratio ω_{ce}/ω_{MW} was approximately 9.3...13.95. The density of the generated plasma was higher than the critical density. For the realization of non-resonant MD in a wide range of values of a magnetic field, the frequency of the generator needs to be changed (replacement of the generator). This is a significant advantage over the ECR method of creating pre-ionized plasma. For ECR discharges, an EC zone in the confinement volume is necessary. This condition is difficult to fulfill without changing the frequency (replacing the generator), in case of a significant change in the magnetic field value in the experiment. Furthermore, the advantage of non-resonant MD is the feasibility of using commercially available microwave generators at a low-power frequency of 2.45 GHz. Pre-ionized plasmas generated

by non-resonant MD can be used not only to initiate NBI but also to initiate radio-frequency (RF) discharges, including the ion-cyclotron frequency range. Thus, it was reported that pre-ionization leads to a decrease in RF breakdown time and increases stability. To date, no comprehensive discussion of non-resonant MD has been presented [12].

In this study, the initial stage of non-resonant MD in Heliotron J was investigated. The study of the initial stage of non-resonant MD is an important step toward understanding the physical processes in the discharge. It is also an important step to further optimize the conditions for the development of plasma pre-conditioning for start-up NBI.

1. EXPERIMENTAL SETUP

This experiment was conducted in a medium-sized helical-axis heliotron device, Heliotron J with the major radius R_0 of 1.2 m, plasma minor radius $<a_p>$ of 0.1...0.2 m and the magnetic field strength at the magnetic axis $B_0 \leq 1.5$ T. The plasma volume is 0.68 m^3 in the standard configuration of Heliotron J [8-11]. To realize a non-resonant microwave discharge on Heliotron J, a generator was used at 2.45 GHz with an output power of up to 20 kW. Microwave power was injected from a rectangular waveguide into a Heliotron J vacuum chamber. The polarization of the microwaves was close to the O-mode.

The linear-averaged electron density was measured using a Mach–Zehnder-type microwave interferometer (130 GHz) based on heterodyne detection [13]. The intensity of the impurity line emission of CIII (464.7 nm) and OV (278.1 nm) was measured with two sets of 25-cm monochromators (NIKON: P250)

equipped with a photomultiplier tube. A radiometer system in a frequency range of 58...74 GHz was used to measure the radiation intensity from non-thermal electrons. Gas fueling was controlled using the pre-programmed piezo-electric valve system. The experimental data were acquired and stored by the data acquisition system of Heliotron J.

2. OVERVIEW OF EXPERIMENTS

Non-resonant microwave discharge studies have been conducted for the magnetic field strength of $B_0 = 1.26$ T along the magnetic axis. The magnetic configuration modified STD (close to STD). In this case, the condition $\omega_{ce}/\omega_{MW} > 1$ is fulfilled in the entire volume of the vacuum chamber. The volume of the vacuum chamber was continuously filled with working gas D_2. The pressure was $5 \cdot 10^{-5}$ Pa. In certain experiments, D_2 was additionally puffing. The duration of injection and the gas flow were adjusted according to the experimental conditions. The microwave power was between 2 and 15 kW. The experimental condition was as follows: The microwave generator was started at -250 ms (Fig. 1). The microwave power was increased to the maximum value for a time of approximately 100 ms (time moment $T_1 \approx$ -150 ms, see Fig. 1). The onset of the injection of fast neutral atoms occurred at approximately 170 ms. The second scenario was similar to the first, except that at time moment $T_2 \approx 17.6$ ms (see Fig. 1), the power injected into the chamber was increased. Accordingly, the power scanning mode was implemented.

3. RESULTS AND DISCUSSION

3.1. START-UP OF NON-RESONANT MICROWAVE DISCHARGES

After non-resonant MD plasma is produced, it undergoes several phases in sequence. The first stage is the breakdown and production of a pre-ionized plasma. The basic breakdown mechanisms can be assumed to remain the same as MD without any magnetic field [14]. The electron avalanche develops independently in each location within the confinement volume, and emission processes from the walls do not play any role. The main difference from MD without a magnetic field, in this case, is the presence of a strong magnetic field and closed flux surfaces. This reduces losses of charged particles due to diffusion, and accordingly breakdown can be realized at extremely low pressures. However, the breakdown in non-resonant MD has not been sufficiently studied.

After the breakdown, the plasma density begins to increase. Two stages are experimentally observed. As can be seen from Fig. 2, both in the case without additional gas puffing and with additional gas puffing, there is a linear and non-linear increase in plasma density. Accordingly, the second stage is an increase in the linear phase of plasma density. A possible main mechanism of plasma formation is the ionization of gas by high-speed electrons that are present in non-resonant MD [9]. Linear density increase continues until time t_1 (see Fig. 2). A further extrapolation of the linear phase

density (see red dashed line in Fig. 2) in time shows the contribution to the total density change owing to only the main linear phase ionization mechanisms.

Starting from time t_1, the third stage begins, that is, the phase of nonlinear increase in plasma density that is characterized by a significant change in the value of dN_e/dt and non-linear increase in plasma density (see Fig. 2). These changes are associated with a change in the basic mechanism of plasma formation.
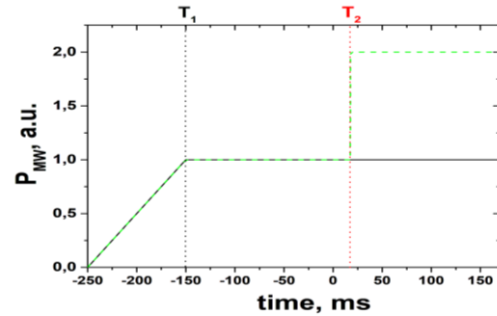
Fig. 1. Plot of time-dependent microwave power
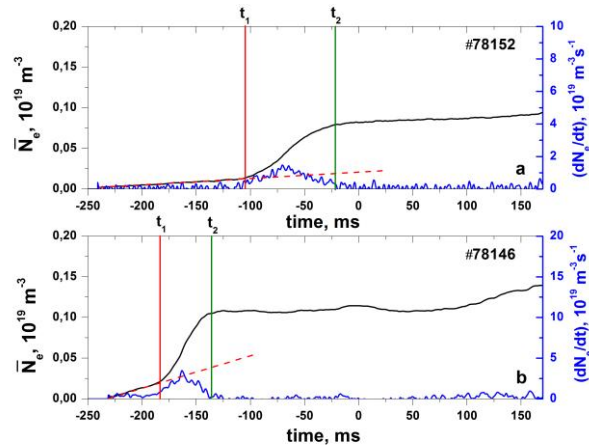
Fig. 2. Time evolution of electron density N_e and dN_e/dt.
No additional gas puffing (a);
additional gas puffing (b), ($P_{MW}(max) = 5$ kW)

Fig. 3,a shows the density reached at time t_1 for different non-resonant MD snatches. Time t_1 was determined from the initiation of the increase in dN_e/dt and graphically from the start of extrapolation of the density of the linear phase (see Fig. 2). The analysis shows that at time t_1, an average density close to critical density N_c or greater than N_c by a factor of approximately 2 is reached. For ordinary waves (O-wave), upon propagation across the plasma column (perpendicular to the magnetic field), the critical density is determined from the condition of equality ω_{pe} of the plasma frequency and ω_{MW} of the microwave frequency $\omega_{pe} = \omega_{MW}$, respectively [5, 15]:

$$N_c = (\omega_{MW}^2 \times m_e \times \varepsilon_0)/e_0^2, \qquad (1)$$

where m_e is the electron mass in kg; e_0 is the charge of an electron in C; ε_0 is the electrical constant; ω_{MW} is the angular frequency of the electromagnetic wave, $\omega_{MW} = 2\pi \cdot f_{MW}$. Accordingly, for a frequency of $f_{MW} = 2.45$ GHz, $N_c = 7.45 \cdot 10^{16}$ m^{-3} (equation 1). When

the density approaches N_c, the refractive index O-wave tends to 0, and the absorption index increases [5, 14]. This leads to an increase in the absorbed microwave power in the plasma. Accordingly, the plasma electrons are heated. This is one possible mechanism for heating electrons.
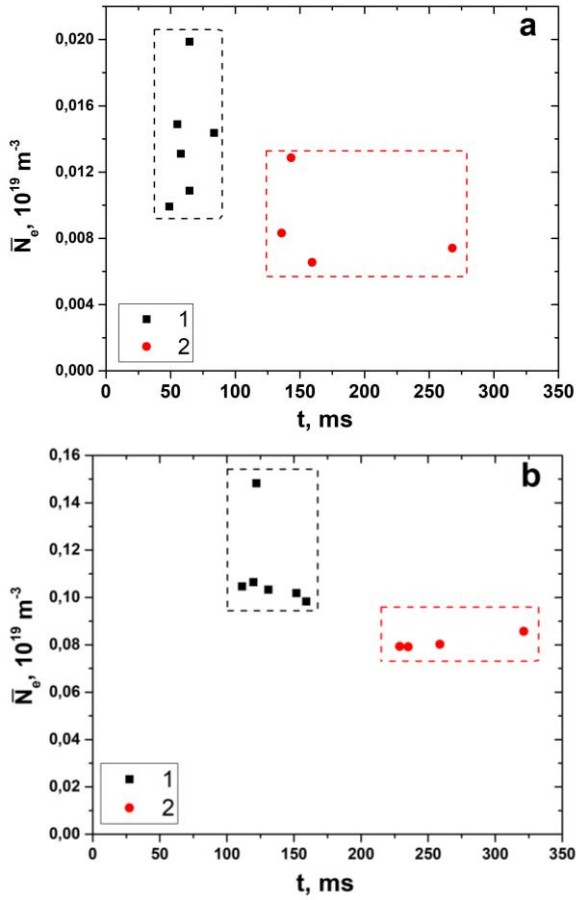
Fig. 3. Dependence of density on the time of t_1 start (a)
and t_2 end (b) of the nonlinear phase.
$t = t_1 + 250$ ms (a), $t = t_2 + 250$ ms (b).
1 – additional gas puffing, 2 – No additional gas puffing

The main mechanism of plasma formation is the ionization of gas by bulk plasma electrons. At a concentration of electrons greater than the critical value, $N_e > N_c$, the wave does not propagate in plasma. In this case, the characteristic depth of field penetration into the plasma is equal to δ skin depth [16]. If thickness l of the plasma layer significantly exceeds this dimension $l \gg \delta$, the electromagnetic wave cannot penetrate through the layer and is reflected from its boundary [16]. The estimate shows that for frequency $f_{MW} = 2.45$ GHz (vacuum wavelength $\lambda_0 = 12.2$ cm), $\delta \approx 12.2$ cm at density $N_e = N_c = 7.45 \cdot 10^{16}$ m^{-3}, and $\delta \approx 1.5$ cm at density $N_e = 2 \cdot 10^{17}$ m^{-3}. Accordingly, for the reflection of electromagnetic waves, the thickness layer with a density equal to or more than N_c should be sufficiently significantly large.

Note that the interferometer measures the average value of plasma density along the length. In the case of a uniform density profile, the maximum density value $N_e(max)$ is $N_e(max)$ = average N_e. A uniform density profile is rarely observed in the experiments. For other density profiles, $N_e(max) >$ average N_e. Reflection,

transmission, and absorption of microwave power for different plasma density profiles have been considered [17]. Therefore, if the condition $l \gg \delta$ ($N_e \geq N_c$) is not satisfied, the electromagnetic wave is partially reflected and transmitted through the plasma, and the microwave power is absorbed in the plasma column. If the condition $l \gg \delta$ ($N_e \geq N_c$) is satisfied, the electromagnetic wave is reflected from the plasma layer with $N_e \geq N_c$, and the microwave power is absorbed in layers with lower density. Apparently, both the cases considered can characterize the time moment t_1.

Electromagnetic waves emitted by a rectangular waveguide can propagate not only directly perpendicular to the plasma and magnetic field lines, but also at an angle to the plasma and magnetic field. At an oblique incident O-wave on the plasma layer, the critical density $N_{c, \psi}$ is determined from the relation [16]:

$$N_{c, \psi} = N_c \times \cos^2\psi, \qquad (2)$$

where ψ is the angle between the wave vector and the normal to the plasma layer (angle of incidence). As can be seen from equation 2, the critical density is lower for an oblique incident O-wave plasma layer than for a perpendicular incident plasma layer. In the case of an electromagnetic wave propagating parallel to the magnetic field, the critical density for a left-hand circularly polarized wave will be determined from the relation [5]:

$$\omega_{pe} = \omega_{MW}(1 + \omega_{ce}/\omega_{MW})^{1/2}, \qquad (3)$$

where ω_{pe} is the plasma frequency, ω_{ce} electron cyclotron frequency. Accordingly, in this case the value of $N_c^L = 1.15 \cdot 10^{18}$ m^{-3} (equation 3) is greater than the value of N_c for O-wave. If $\omega_{ce} > \omega_{MW}$ right-hand circularly polarized waves can also propagate and is called whistlers modes. It is noted for cases $N_c > N_e$ that the low absorption causes multiple reflections of the microwave in the vessel. It leads to multipass absorption and a microwave propagation and polarization mixture. In cases $N_e > N_c$ multiple reflections and polarization changes are also possible. All of these mechanisms can also lead to absorption and heating of electrons.

The value of time t_1 is less for the scenario with additional gas puffing than that in the scenario without gas puffing. The plasma density achieved is higher in the scenario with additional gas puffing. With additional pulsed gas puffing, the gas pressure and the corresponding number of neutral molecules (atoms) increase. This leads to an increase in the probability of collision of electrons with the molecule (atoms) and ionization. In this case, the time of reaching the plasma density of the order of N_c decreases, and the achieved plasma density increases.

The fourth stage begins after time t_2. At this stage, the quasi-stationary stage, the density does not change substantially. Fig. 3,b shows the density reached at time t_2 for different non-resonant MD scenarios. The achievable average density is substantially greater than N_c. Accordingly, the size of the layer with $N_e > N_c$ becomes significant. Microwave power is reflected from the peripheral plasma layers and does not propagate into the plasma volume. The plasma density is determine

from the balance between the formation of charged particles and their losses.

3.2. NON-RESONANT MICROWAVE DISCHARGES

Previously, non-resonant MD was investigated on Heliotron J [8-11] only in plasma production regimes at $P_{MW} = $ const. Therefore, the two modes with $P_{MW} = $ const and microwave power scanning were compared. Fig. 4 shows the dependence of the electron cyclotron emission (ECE) intensity, CIII spectral line emission, and average density on time. Regarding the dependence of average plasma density on time, two main regions can be conventionally distinguished. The first region shows an increase in plasma density up to a certain value that is approximately 20% lower than the maximum density achieved in the shot. The second is the quasi-stationary region. The plasma density changes insignificantly in this area. The maximum intensity of ECE radiation and spectral line CIII is observed in the quasi-stationary region of average plasma density. A similar situation is observed in the case without additional working gas puffing. In the case of an increase in the microwave power at time T_2, e.g., from 5 to 10 kW (see Fig. 4, shot № 78147), the plasma density increases. The density increase to the maximum value occurs rather smoothly within approximately 130 ms. Thus, the maximal plasma density reached in this case is higher than that at $P_{MW} = $ const (see Fig. 4, shot № 78148).

The maximum average plasma density achievable in a non-resonant microwave discharge increases with increasing microwave power, as can be seen in Fig. 5. This dependence has been previously observed [7, 9]. When using additional gas puffing with increasing injected power, the maximum value of plasma density increases more significantly than in the case without additional gas. In the case of the mode with power scanning, the maximum density reached in the experiment is slightly higher than that at $P_{MW} = $ const.

In the case of the power-scanning regime, the density increase is delayed with respect to the timemoment T_2 of the microwave power increase (see Fig. 4, shot № 78147). Therefore, to optimize the conditions for producing the maximum plasma density in the power scanning regime, experiments were conducted with changes in the modes of additional gas injection. Fig. 6 shows the intensity I_{ECE} and spectral line CIII, average electron density N_e for different scenarios of additional gas puffing. An increase in the gas by 50 ms leads to an increase in the plasma density (see Fig. 6,a,d, shot № 78149). Simultaneously, the beginning of plasma density increase occurs with a small delay of approximately 20 ms relative to the start of the gas puffing increase. Comparison of shots № 78147 and 78149 after time T_2 when $P_{MW}(max) = $ 10 kW shows that increasing the gas puffing (pressure increase) can change the maximum achievable density in non-resonant MD.

In shot № 78150 (see Fig. 6), the start time of gas increase has been shifted to the region when $P_{MW}(max) = $ 5 kW. Consequently, the plasma density up to time T_2 practically did not change. The intensity of the CIII line decreased to almost zero after the onset of an increase in gas puffing. This is due to a decrease in the electron temperature of the plasma. After an increase in power $P_{MW}(max)$ up to 10 kW over time T_2, a rapid increase in plasma density and CIII line intensity is observed. Accordingly, by changing the additional gas puffing and microwave power, a higher plasma density is feasible.
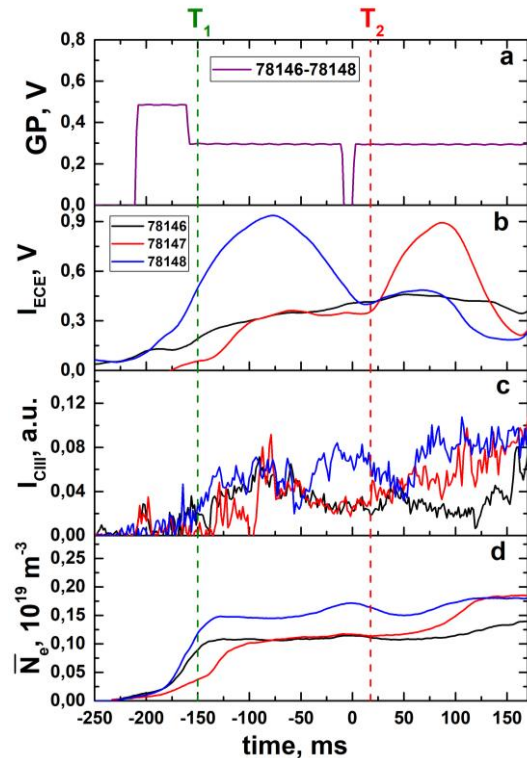
Fig. 4. Time evolution of additional gas puffing GP (a), radiometer intensity I_{ECE} (b), intensity spectral line CIII (c), and average electron density N_e (d); (shots: #78146 $P_{MW}(max) = 5$ kW, #78148 $P_{MW}(max) = 10$ kW, #78147 $P_{MW}(max) = 5...10$ kW). T_1 – the point in time when the maximum microwave power is reached, T_2 – the time moment of increasing microwave power (only for shot #78147)
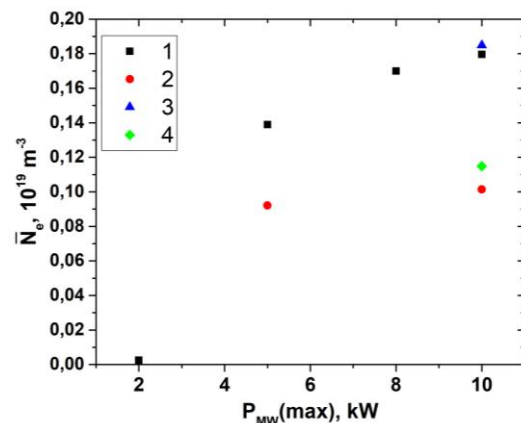
Fig. 5. Maximum average electron density as a function of microwave power (time = 165 ms). 1 – additional gas puffing; $P_{MW}(max) = $ const; 2 – № additional gas puffing, $P_{MW}(max) = $ const; 3 – additional gas puffing, scanning power $P_{MW}(max) = 5...10$ kW; 4 – № additional gas puffing, $P_{MW}(max) = 5...10$ kW
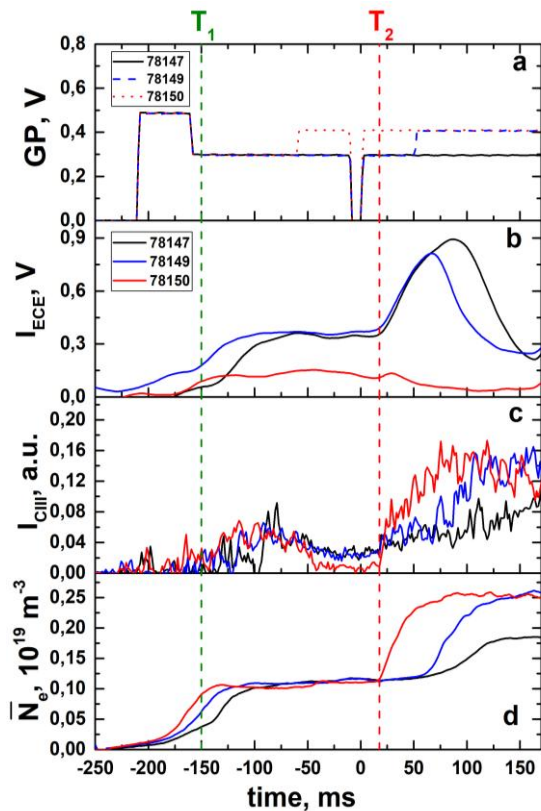
Fig. 6. Time evolution of additional gas puffing GP (a), radiometer intensity I_{ECE} (b), intensity spectral line CIII (c), and average electron density N_e (d). (Additional gas puffing, $P_{MW}(max)$=5...10 kW). T_1 – the point in time when the maximum microwave power is reached, T_2 – the time moment of increasing microwave power
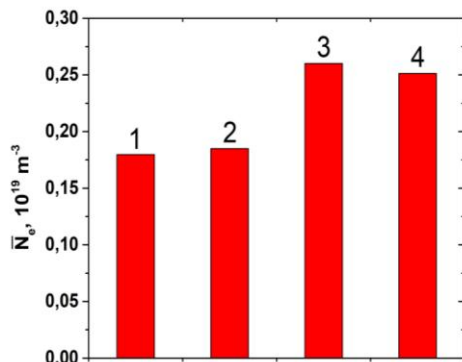
Fig. 7. Maximum average electron density (time = 165 ms). Additional gas puffing:
1 – $P_{MW}(max)$ = 10 kW (shot № 78148);
2 – $P_{MW}(max)$ = 5...10 kW (shot № 78147);
3 – $P_{MW}(max)$ = 5...10 kW (shot № 78149);
4 – $P_{MW}(max)$ = 5...10 kW (shot № 78150)

Fig. 7 summarizes the results obtained for different scenarios of microwave power input and additional gas injection. In Scenario № 3, the maximum plasma density is attained with the same value for all scenarios with a puffing microwave power of 10 kW.

As shown through the experiments in Heliotron J [9], WEGA [18], and TJ-K [19], several groups of electrons with different energies are observed in the non-resonant MD plasma. In the first case, bulk plasma electrons with temperatures ranging from a few tens to hundreds of electron volts. The second group of high-speed electrons exhibit energies up to several megaelectronvolt. The exsistence of high-speed electrons is confirmed by x-ray, radiometer intensity, and γ-ray emission measurements [9]. High radiometer intensity is also observed in these experiments (see Figs. 2 and 4). The presence of the observed radiometer signal is explained by synchrotron radiation emitted by high-speed relativistic electrons. Mechanisms of high-speed electron formation are discussed [9, 18-20]. A possible mechanism for the formation of high-speed electrons may be the acceleration of electrons in stochastic electric fields [18, 20]. Note that in the presence of fluxes of high-speed electrons in the plasma, the development of instabilities in plasma is possible [21]. As a result of the interaction of the plasma beam, additional heating of plasma bulk electrons is possible [22]. Regardless of the mechanism of electron heating, the maximum plasma density is determined by the balance of charged particle generation and their losses.

Depending on the experimental conditions and the scenario for the non-resonant MD, two cases can be conventionally distinguished. In the first case, non-resonant MD achieves a maximum density below the critical density $N_e < N_c$. In the second case, the plasma density is higher than the critical density $N_e > N_c$. As can be observed from Figs. 5 and 7, the experimentally achieved maximum plasma density is higher than N_c.

Thus, it is possible to achieve a higher plasma density in the non-resonant MD regime with power scanning than in the constant-power regime. However, optimization of this mode is still required. Furthermore, an additional lever to control plasma parameters in the discharge is preferred in the additional gas puffing scenario.

CONCLUSIONS

Investigations of non-resonant microwave discharges showed that several stages can be differentiated in the discharge: breakdown and formation of pre-ionized plasma, linear and nonlinear phases of plasma density increase, and quasi-stationary stage. The maximum average density achieved in the experiments is substantially greater than $N_c = 7.45 \cdot 10^{16}$ m^{-3} and can reach the value of $2.5 \cdot 10^{18}$ m^{-3}. In the power-scanning mode in non-resonant microwave discharges, it is possible to achieve a higher plasma density than in the constant-power mode. By preferring additional gas injection and microwave power, achieving higher plasma densities is feasible.

ACKNOWLEDGEMENTS

REFERENCES

1. C.M. Ferreira, M. Moisan / Edited by. *Microwave Discharges Fundamentals and Applications.* New York: "Springer", 1993, 564 p.

2. N. Sakudo. Microwave ion sources for industrial applications // *Review of Scientific Instruments.* 2000, v. 71, № 2, p. 1016-1022.

3. Yu.A. Lebedev. Microwave discharges at low pressures and peculiarities of the processes in strongly non-uniform plasma // *Plasma Sources Sci. Technol.* 2015, v. 24, № 5, p. 053001.

4. B. Lloyd. Overview of ECRH experimental results // *Plasma Phys. Control. Fusion.* 1998, v. 40, № 8A, p. A119-A138.

5. G. Guest. *Electron Cyclotron Heating of Plasmas.* Weinheim: "Wiley-VCH", 2009, 253 p.

6. V. Kopecky, J. Musil, F. Zacek. Absorption of microwave energy in a plasma column at high magnetic fields // *Physics Letters A.* 1974, v. 50, № 4, p. 309-310.

7. V. Kopecky, J. Musil, F. Zacek. Absorption of electromagnetic waves in a radially inhomogeneous plasma at high magnetic fields // *Plasma Physics.* 1975, v. 17, № 12, p. 1147-1153.

8. S. Kobayashi et al. Plasma startup using neutral beam injection assisted by 2.45 GHz microwaves in Heliotron J // *Nucl. Fusion.* 2011, v. 51, № 6, p. 062002.

9. S. Kobayashi et al. Study of seed plasma generation for NBI plasma start-up using non-resonant microwave launch in Heliotron J // *Plasma Phys. Control. Fusion.* 2020, v. 62, № 6, p. 065009.

10. S. Kobayashi, et al. Study of NBI Plasma Start-Up Assisted by Seed-Plasma Generation using Nonresonant Microwave Heating in Heliotron J // *28th IAEA Fusion Energy Conference* 10-15 May 2021. *Programme and List of Contributions and Linked Conference Materials.* EX/P6-36, p. 362.

11. S. Kobayashi et al. Role of pre-ionization in NBI plasma start-up of Heliotron J using non-resonant microwave heating // *Nucl. Fusion.* 2021, v. 61, № 11, p. 116009.

12. V.E. Moiseenko et al. Radio-frequency plasma start-up at Uragan-3M stellarator // *Problems of Atomic Science and Technology. Series "Plasma Physics" (107).* 2017, № 1, p. 54-59.

13. Y. Ohtani et al. Gas puff modulation experiment measured by interferometers in Heliotron J // J*ournal of Instrumentation.* 2016, v. 11, p. C02035.

14. Y.P. Raizer. *Gas Discharge Physics.* Berlin: «Springer-Verlag», 1991, 449 p.

15. V.L. Ginzburg. *Propagation of Electromagnetic Waves in Plasma.* Oxford:«Pergamon Press», 1971, 535 p.

16. V.E. Golant. *Microwave Methods of Plasma Diagnostics.* M.: "Nauka", 1968, 238 p.

17. G.R. Nicoll, J. Basu. Reflection and transmission of an electromagnetic wave by a gaseous plasma // *Proceedings of the IEE – Part C:* Monographs. 1962, v. 109, № 16, p. 335-348.

18. H.P. Laqua et al. Stochastic acceleration of relativistic electrons and plasma heating and current drive with 2.45 GHz frequency at the WEGA stellarator // *Plasma Phys. Control. Fusion.* 2014, v. 56, № 7, p. 075022.

19. A. Köhn-Seemann et al. Plasma electron acceleration in a non-resonant microwave heating scheme below the electron cyclotron frequency // *New J. Phys.* 2022, v. 24, № 6, p. 063024.

20. V. Fuchs et al. Relativistic Fermi-Ulam map: Application to WEGA stellarator lower hybrid power operation // *Physics of Plasmas.* 2014, v. 21, № 6, p. 061513.

21. Ya.B. Fainberg. The interaction of charged particle beams with plasma // *J. Nucl. Energy, Part C Plasma Phys.* 1962, v. 4, № 3, p. 203-220.

22. L.D. Smullin. A Review of the Beam Plasma Discharge // *Relation between laboratory and space plasmas.* Dordrecht, Holland, 1981, p. 45-64.

ІНІЦІЮВАННЯ НЕРЕЗОНАНСНОГО МІКРОХВИЛЬОВОГО РОЗРЯДУ В ГЕЛІОТРОНІ J

Ю.В. Ковтун, K. Nagasaki, S. Kobayashi, T. Minami, S. Kado, S. Ohshima, Y. Nakamura, A. Ishizawa, S. Konoshima, T. Mizuuchi, H. Okada, H. Laqua, T. Stange

Досліджено нерезонансний мікрохвильовий розряд у сильних магнітних полях, коли виконується умова $\omega_{ce}/\omega_{MW} > 1$ (ω_{ce} та ω_{MW} кутова електронна циклотронна частота та кутова мікрохвильова частота відповідно). При формуванні плазми нерезонансного мікрохвильового розряду послідовно проходять декілька фаз: пробій і утворення попередньої плазми, лінійна і нелінійна фази збільшення густини плазми, квазістаціонарна стадія. Досліджено декілька режимів нерезонансного мікрохвильового розряду. У режимі сканування потужності в нерезонансному мікрохвильовому розряді можна досягти більшої густини плазми, ніж у режимі постійної потужності. Максимальна середня густина, досягнута в експериментах, істотно перевищує критичну густину для О-хвилі (звичайної хвилі) $7{,}45\cdot10^{16}$ м$^{-3}$ і може досягати значення $2{,}5\cdot10^{18}$ м$^{-3}$.